Kalra Ajay (Orcid ID: 0000-0003-3878-2346)

Climatic variability of the Pacific and Atlantic Oceans and western U.S. snowpack

Pratik Pathak[1], Ajay Kalra[2*], Kenneth W Lamb[3], William Paul Miller[4], Sajjad Ahmad[5], Rajesh Amerineni[6], and Devi Priya Ponugoti[6]

[1]FTN Associates, Ltd., Little Rock, AR.

[2]Department of Civil and Environmental Engineering, Southern Illinois University, 1230 Lincoln Drive, Carbondale, IL.

[3]Department of Civil Engineering, California State Polytechnic University Pomona, Pomona, CA.

[4] NOAA Colorado Basin River Forecast Center, Salt Lake City, UT.

[5]Department of Civil and Environmental Engineering and Construction, University of Nevada, Las Vegas, 4505 S. Maryland Parkway, Las Vegas, NV.

[6]Department of Electrical and Computer Engineering, Southern Illinois University, 1230 Lincoln Drive, Carbondale, IL.

*Corresponding Author

Abstract

This study examines the changing characteristics of snow water equivalent (SWE) in western U.S. and their teleconnections with large-scale variability of the Pacific and Atlantic Oceans. This study evaluated the relationship among sea surface temperatures

This is the author manuscript accepted for publication and has undergone full peer review but has not been through the copyediting, typesetting, pagination and proofreading process, which may lead to differences between this version and the Version of Record. Please cite this article as doi: 10.1002/joc.5241

(SST), 500-mbar geopotential height (Z_{500}), 500-mbar east-west wind (U_{500}), and western U.S. SWE (1 March, 1 April, and 1 May). The averages of SST, Z_{500} and U_{500} were computed to create a lead time of 2 to 10 months. Three different six-month series were computed – January- June, April-September, and July-December – and were correlated with SWE stations in the western U.S. The study utilized singular value decomposition (SVD) for a period of 1961-2016 to correlate the SWE and climate indices. SVD was applied between the standardized SST and SWE to obtain their correlation and to evaluate connection with Z_{500} and U_{500} within the same SVD relationship. Specifically, SVD was not applied independently on each variable prior to this study. The correlations were observed to increase as the lead time decreased. First mode SVD showed a pronounced non-ENSO short-wave train for the July-December climate in the Z_{500} data; this terminated over the Great Lakes region, and was strongly correlated with the warming of the SST near the east coast of Japan, resulting in decreased SWE in the study area. Second mode SVD showed a negative correlation between SWE stations in Colorado and Utah and SST near the Asian and Australian continents. The associations between climate indices and SWE that were identified during this study could be used to improve long-term forecasts, resulting in better management of water resources in the region.

Keywords:

sea surface temperature, snow water equivalent, singular value decomposition, geopotential height, east-west wind

Introduction

Understanding variations in atmospheric circulation is important when determining spatial and temporal changes in hydrologic variables. Due to climate change, changes to the global atmospheric circulation have considerable effects on water resources worldwide (Pachauri et al., 2014). Climate change invariably affects the global and regional hydrological cycles, and the assessment of future change in hydrology is associated with a high degree of uncertainty (Hagemann et al., 2013; Thakali et al., 2016). According to Trenberth (2011), the intensity and frequency of precipitation is altering; subsequently, the severity of extreme hydrological events is imminent in near future. One such example is the increasing variability of streamflow as well as other changes to the hydrologic cycle (Stephen et al., 2010). It has become essential to understand the effects of atmospheric variability on spatio-temporal characteristics of streamflow in order to properly manage water resources (Lempert and Groves, 2010; Pathak et al., 2016a; Tamaddun et al., 2016).

An important part of annual hydrological cycle and a major source for runoff and water supply is snow in the mountainous region of western U.S. (Scalzitti et al., 2016, Tamaddun et al., 2017a). Precipitation is mostly dominated by snowfall in winter in these regions. An increase in winter and spring temperatures may result in increased streamflow during winter and reduced flow during summer, along with- a decrease in the snow-water equivalent (Hamlet et al., 2005; Pathak et al., 2016b). Several studies have shown a

reduction in snowpack in the western U.S. (Mote et al., 2005; Hamlet et al., 2005). The decline is much more conspicuous in northern regions because of higher elevations and high sensitivity to temperature (Pederson et al., 2011). Safeeq et al. (2015) studied the effects of climate variability on the proportion of snow to precipitation in the western U.S., and concluded that a higher sensitivity to climate change was observed in more recent times as compared to the past.

Studies have evaluated the response of streamflow and precipitation with oceanic-atmospheric variability across the continental United States (Cayan and Peterson, 1989; Kahya and Dracup, 1993; Aziz et al., 2010). The western U.S. has demonstrated a streamflow variability that is correlated with the El Niño- Southern Oscillation (ENSO) (Cayan and Peterson, 1989; Kahya and Dracup, 1993; Tamaddun et al., 2017b), Pacific Decadal Oscillation (PDO) (Hunter et al., 2006), and Atlantic Multidecadal Oscillation (AMO) (e.g., Enfield et al., 2001). At interannual time scales, ENSO dominates the variability of winter precipitation across North America (Ting and Wang, 1997). At decadal and multidecadal time scales, PDO (Mantua et al., 1997) and AMO (Tootle and Piechota, 2006) are two important teleconnections that drive the variability of precipitation across the United States.

Additional studies have argued about the teleconnections of decadal variabilities of oceanic atmospheric parameters with regard to the hydrology of different region (Li et al., 2015; Dettinger and Diaz, 2000). Wang et al. (2012) studied teleconnection pattern of multi-decadal drought variability between Great Basin, which extends through most of Nevada and several contiguous states, and warm-cool phases of interdecadal Pacific Oscillation. McCabe and Dettinger (1999) demonstrated that the variation in ENSO strength was teleconnected with the precipitation of western United States. Further, Zhang and Delworth (2007) have argued for the contribution of AMO to variations in PDO and ENSO components, suggesting the simultaneous teleconnection of both Pacific and Atlantic variabilities with western U.S. hydrology.

Several studies have presented the possibility of a predefined variability in sea surface temperature (SST) to explain oceanic-atmospheric phenomena (e.g., the tropical Pacific Ocean and the northern Atlantic Ocean). Predefining SST regions may lead to spatial bias or limit the scope of study such that important interactions are missed. Taking into consideration the entire Pacific Ocean and Atlantic Ocean could lead to identification of new SST regions that affect western streamflow variability (Tootle and Piechota, 2006).
Along with SST, oceanic-atmospheric climate variability can be influenced significantly by various mechanisms at certain air-pressure zones. Several studies have identified the 500-mbar geopotential height (Z_{500}) as a predictor variable that effectively predicts the snow

water equivalent (Grantz et al., 2005; Oubeidillah et al., 2011). The geopotential height is defined as the height of the pressure surface measured above the mean sea level while recording the actual observation. Oubeidillah et al. (2011) used a region of Z_{500} in Upper Colorado River and Great Basin, and concluded that Z_{500} improved short-lead time (three-month) forecasts. Similarly, Grantz et al. (2005) used Z_{500} as well as SWE to improve seasonal forecasting in the Truckee-Carson River System, and concluded that and index using 500-mbar geopotential height reasonably improved the forecasting accuracy when compared to using SWE alone. In addition to SST and Z_{500}, wind stress is another parameter utilized by several studies to predict rainfall (e.g., Munot and Kumar, 2007). The U-wind stress (eastward wind at 500 hPa, U_{500}) is the force applied by the wind per unit area parallel to the surface of large bodies of water at different levels of pressure.

Various methods are available to determine such relationship variables as SST, Z_{500}, U_{500}, and SWE. Bretherton et al. (1992) compared four different methods and concluded that SVD was the easiest method to implement as well as being superior to the other methods. Thereafter, various studies have employed SVD to understand the interdependency among SST and Z_{500} with streamflow and precipitation variability across the U.S. (Uvo et al., 1998; Wang and Ting, 2000; Aziz et al., 2010; Sagarika et al., 2015a, b). Tootle and Piechota (2006) applied the SVD technique to identify the significant SST regions that correlated with U.S. streamflow. The study attributed the variation in

streamflow to ENSO and PDO signanls in Pacific Ocean and AMO signal in Atlantic Ocean. They concluded that the integration of PDO, ENSO, and AMO – along with other climatic signals – resulted in strong associations with streamflow in the United States. Aziz et al. (2010) utilized the SVD technique to identify the influence of the Pacific Ocean SST on snowpack of the Upper Colorado River Basin (UCRB). They identified the Pacific Ocean SST region between 34° N-24 ° S and 150° E to 160° W as the most consequential driver of the UCRB snowpack. Recently, Ao et al. (2015) used SVD to study variations in snow cover in Eastern Europe caused atmospheric variability.

The need to manage the available water resources and make decisions in advance necessitates the understanding of the factors that drive snowpack in western United States. Therefore, the objectives of this current study were to understand:

1. The teleconnections of western U.S. with the Atlantic Ocean in addition to the Pacific Ocean.
2. The interactions of SST, Z_{500}, and U_{500}; and find new significant regions that drive the SWE in the western United States.

The goal of the present research was to evaluate the spatio-temporal relationships among three climate indicators for long-term variability: SST, geopotential height (Z_{500}), zonal wind (U_{500}), and western U.S. SWE.

SVD analysis for a period of 56 years 1961 (-2016) was performed to determine interannual and interdecadal variations for both Pacific and Atlantic Ocean influences. The SVD used in this study correlates SWE with multiple parameters by preserving information of the first variable while correlating new variables. Unlike previous studies (Aziz et al., 2010; Sagarika et al., 2015 a, b), which performed SVD analyses between the climate indices and streamflow/ snowpack separately, this current study performed SVD between SST and SWE. The temporal expansion series (TES) that was created was directly correlated with standardized Z_{500} and U_{500} data so as to preserve the initial relationship between SST-SWE. This procedure was adopted so as to observe the connections of Z_{500} and U_{500} within that relationship. Statistically significant correlation values (95% level) in the heterogeneous matrices then were mapped.

This study significantly extends the work of Aziz et al. (2010) by utilizing SVD analysis when considering updated climate fields (Z_{500}, and U_{500}); it also incorporated Atlantic Ocean influences on western U.S. snowpack variability. It was very essential to understand the changes in SWE when considering the three variables together, as they are dependent on one another and drive the SWE into the basin. For example, when temperatures get warmer in one region, this may cause an atmospheric dipole that shifts the jet stream to the north or south. Another example is that warming SSTs in one region may be correlated with a high pressure dome that affects wind intensity in another region.

Study Area and Data

Historic SWE data for 1 March, 1 April, and 1 May for the period of 1961 to 2016 (56 years) were obtained from the Natural Resources Conservation Service website of the U.S. Department of Agriculture for monthly snow data (http://wcc.sc.egov.usda.gov/nwcc/rgrpt?report=snowcourse&state=co). SWE data for 291 1 March snowpack stations, 322 1 April stations, and 215 1 May stations were identified after the tradeoff was determined between its spatial and temporal availability. The nature of the snowpack data in the western U.S. is discussed briefly by Serreze et al., (1999). Previous research used SWE data utilizing SVD with SSTs and Z_{500} (Tootle and Piechota, 2006; Aziz et al., 2010). The spatial variation of 1 March, 1 April, and 1 May snowpack stations in the western U.S. are illustrated in Figure 1. A limited number of Snow Telemetry (SNOTEL) stations are located in the southwestern U.S., as seen in Figure 1, because the hydrology there is driven less by snowpack and the resulting snowmelt and more by convective precipitation events, typically realized as rainfall events.

In addition to snowpack stations, monthly SST, Z_{500}, and U_{500} data were obtained from a website from the Earth System Research Laboratory, Physical Sciences Division , of the National Ocean and Atmospheric Administration (http://www.esrl.noaa.gov/psd/data/gridded/data.ncep.reanalysis.derived.pressure.html) for the period from 1960 to 2015 (56 years). The SST, Z_{500}, and U_{500} dataset were obtained for

the Pacific Ocean within the region of 100° E to 80° W and 30° S to 70° N and for the Atlantic Ocean within the region of 80° W to 20° W and 30° S to 70° N. The resolution of the gridded data for the average monthly oceanic SST was 2° × 2°, and Z_{500} and U_{500} both were 2.5° × 2.5°. The total number of gridded SST cells obtained were 3432 in the Pacific Ocean and 1149 in the Atlantic Ocean; the gridded Z_{500} and U_{500} cells were 2988 in the Pacific and 1025 in the Atlantic Ocean. In the current study, the SST, Z_{500}, and U_{500} for both the Pacific and Atlantic Ocean were averaged for three different six-month series: January to June (Jan-Jun), April to September (Apr-Sep), and July to December (Jul-Dec).

Methodology

SVD is a powerful statistical tool with an ability to convey important theoretical and geometrical insights about linear transformations (Kalman, 1996). One of the advantages of using SVD is its robustness in explaining the mean squared temporal covariance between two fields (Bretherton et al., 1992). SVD is capable of identifying the pairs of spatial patterns between two data fields with the maximum possible fraction of the cumulative squared covariance between the time series of the two fields (Yang and Lau, 2004). For a detailed description of the SVD method, refer to Bretherton et al. (1992) and Kalman (1996).

SVD is a factorization matrix comprising of 3 matrices. If there is a symmetric real matrix of the order $n \times n$, there is an orthogonal matrix V and a diagonal D such that $A = VDV^T$.

For SVD, if A is an arbitrary real matrix of the order $m \times n$, then A can be written as $A = USV^T$, where U is $m \times m$ and V is $n \times n$. The eigenvalues of S are in order of decreasing magnitude, and represent the singular values of A. The columns of U and V are referred to as the left and right temporal expansion series (TES) of A.

The relative importance of each mode in the decomposition can be compared by computing the squared covariance fraction (SCF), expressed as:

$$SCF_k = S_k^2 \Big/ \sum_i^r S_i^2 \qquad (1)$$

where S_k is the singular value of the k^{th} mode. For a given mode, the square of any singular value is indicative of the fraction squared covariance between two fields accounted for by that mode. A study by Newman and Sardeshmukh (1995) showed that SVD was useful to determine the correlation between two variables if the percentage of covariance was explained by the first three leading modes or if the columns U S V from the SVD analyses were large and significant.

Similar to *SCF*, the quantification of strength of modes obtained from different SVD expansions can be done by calculating normalized squared covariance (*NSC*) which is given by:

$$NSC = \left(\frac{SS^2}{N_S * N_Z} \right) \quad (2)$$

where SS is the sum of squares of the singular value and N_S and N_Z are the number of snow stations and SST (Z_{500}) grid points, respectively. The NSC value varies between 0 and 1, depending upon the spatial relationship between the two fields. The closer the NSC value is to 1 indicates a higher correlation between the fields.

In the present study, SVD only is applied to the cross-covariance matrix generated using standardized SST anomalies and standardized SWE anomalies. The application of SVD results in the generation of two orthogonal matrices, referred to as the left and right matrices, and a singular valued matrix. The significant spatial relationships between the left (SST) matrix and right (SWE) matrix of singular vectors were examined by correlating the first column, or mode, of the left TES (right TES) with the standardized SWE (SST) anomalies matrix. This produced a heterogeneous correlation matrix for each field, SST as well as SWE.

To analyze the correlation between Z_{500} and U_{500} with SWE, SVD analysis for each of these climate inputs were not repeated. The standardized Z_{500} and U_{500} were directly correlated with the right TES obtained by performing SVD analysis on the standardized SST data and standardized SWE data. The application of SVD on both the SST and SWE data created a

left TES and right TES; embedded in it was the relationship between SST and SWE. The application of SVD separately for Z_{500} -SWE and U_{500} -SWE resulted in losing the SST-SWE relationship, and created a new relationship. In order to preserve the initial relationship between SST-SWE and observe the connection of Z_{500} and U_{500} within that relationship, instead of performing the SVD analysis separately, the right TES created by performing the SVD between SST-SWE was directly correlated with standardized Z_{500} and U_{500} data. Statistically significant correlation values (95% level) in the heterogeneous matrices then were mapped.

The effectiveness of SVD for correlating spatiotemporal data matrices of various dimensions already has been verified (Hunter et al., 2006; Tootle et al., 2008; Soukup et al., 2009;). These studies obtained the correlation with gridded datasets of varying numbers of grid cells, and were able to provide the anticipated climate signals. Based on the literature, SVD also could be incorporated in this current study, even though the number of grid cells for SST was higher than for Z_{500} and U_{500}.

Results and Discussion

The significantly correlated regions for SST, Z_{500}, and U_{500} with SWE for the months of March, April and May are described in this section. Spatial maps for the first mode of 1 March, 1 April and 1 May snowpack stations for SST, Z_{500}, and U_{500} at $p \leq 0.05$ are shown in Figs. 2 through 7. The maps show regions that are significantly correlated with

snowpack stations. The regions with a positive sign (i.e., increasing) identified for SST/ Z_{500}/ U_{500} indicates a positive correlation with the snowpack stations, and vice versa. Table 1 provides a concise summary of the SCF and NSC values.

1 March Snowpack and Pacific Ocean SST, Z_{500}, and U_{500} (First Mode)

Figure 2 shows the correlation maps between significant regions of Pacific Ocean SST, Z_{500} and U_{500} and western U.S. 1 March snowpack at different predictor periods. As the lead time increase between the predictor (i.e., various SST periods) and predictands (i.e., 1 March snowpack stations), the SCF values for the first mode and second mode decrease. The first mode results in SCF values of 49.25%, 67.80%, and 76.65% and the second mode results in SCF values of 26.09%, 11.39%, and 9.55% for the SST of Jan-Jun (the first predictor period), Apr-Sep (the second predictor period), and Jul-Dec (the third predictor period), respectively. Similarly, the NSC values of 1.78, 2.56, and 3.24 were obtained for the first, second, and third predictor periods of SST, respectively. One thing to be noted in Figure 2 is the 'switching' of the signs, as shown in Figures 2a and 2b; this switch is inherent to SVD. The nature of the relationship, either positive or negative, between the predictors and the predictands is important, as indicated by Figure 2.

Figure 2a shows the results for January to June climate input from the previous year (1960 to 2015) with the current year's March 1 SWE observations. This analysis revealed SST-1, a region of increasing SSTs near the ENSO area, along with SST-3, an additional SST band

along the midlatitudes in the central Pacific Ocean. SST warming in these regions appears to be associated with a high pressure ridge (Z-1) over the central/eastern part of North America. In turn, this diminishes the equatorial westerlies (U-3) and strengthens the North American jet stream (U-4). The connections resulted in decreased SWE observations across the study area.

Figure 2b shows that for the April - September climate, decreased SSTs in the Niño 3.4 region (SST-1) resulted in increasing SWE in the study area; this was accompanied with an anomalous low pressure over the study region (Z-3), decreasing pressure over the Alaska (U-4), and decreased equatorial westerlies (U-3). Figure 2c shows a typical ENSO effect during which decreasing SSTs (SST-1) in the equator result in increasing precipitation in the study area. ENSO effects are associated with an atmospheric shortwave train (shown as a red dashed line) that is associated with the Aleutian low pressures over the northwestern United States. Li et al. (2015) studied the decadal variation of the Eastern Pacific and North Pacific on the precipitation of Vietnam, and identified a significant oscillation pattern that has ENSO-like tropical Pacific variability.

Three significant SST regions in the Pacific Ocean were detected for all the predictor periods, and were significantly correlated with snowpack stations in the western United States. The first region was along the eastern equatorial Pacific Ocean residing in the

ENSO belt, and conformed to the Niño 3.4 region. With decrease in lead time, the region intensified; moreover, the correlation was much stronger than the periods with a longer lead time.

Trenberth (1997) defined the region along the equatorial Pacific Ocean between 5^{o} S - 5^{o} N and 170^{o} W - 120^{o} W as the Niño 3.4 SST region. This current study shows significant correlation with the SST anomalies in that region with snowpack in the western United States. The warm phase of ENSO may drive the winter precipitation, and may induce anomalous snowpack pattern across western U.S. (Jin et al., 2006). The ENSO-like region detected showed a significant negative correlation with snowpack in the Pacific Northwest (Washington, Oregon and Idaho) such that warming of the region led to a decrease in snowpack, and vice-versa. This is in agreement with a study by Aziz et al. (2010), which showed a similar result. Other studies have shown that a decrease in precipitation in the Pacific Northwest was significantly correlated with warmer-than-average SST in the ENSO belt (Redmond and Koch, 1991).

When considering all three lag intervals together, increased SWE observations were linked with the development of warming equatorial SSTs, a strengthened shortwave train involving the Aleutian Low, and an increased jet stream entering the northwestern United States. These conditions were preceded by cooling in the equatorial SSTs during the prior

year. This was associated with a shifting of alternating low- and high-pressure regions within the eastern and western U.S., respectively. These changes were accompanied by increased equatorial westerlies during the prior year.

1 March Snowpack and Atlantic Ocean SST, Z_{500}, and U_{500} (First Mode)

Figure 3 shows the correlation maps between significant regions of the Atlantic Ocean SST and western U.S. 1 March snowpack at various predictor periods. The Atlantic Ocean SST variability results in SCF values of 68.91%, 68.87%, and 75.89% for the first mode and 14.60%, 15.26%, and 11.39% for the second mode for various predictor periods. Similarly, the analysis provided NSC values of 2.43, 2.28, and 2.67 for the three SST predictor periods.

Figure 3a shows that for the January – June climate, SST increased in the region, spanning 60˚ W to 30˚ W and 30˚ N to 45˚ N. SST-2 is associated with pressure dipole (Z-1 and Z-2) as well as increasing equatorial westerlies (U-2) and decreasing jet streams (U-1). These connections result in decreased SWE across the study area. Figure 3b shows that the increase in SWE across the study region was correlated with a decreasing SST for the April - September climate across the central Atlantic (SST-3), accompanied by decreasing pressure in the central Atlantic (Z-1) and decreasing wind stresses over the South American continent (U-1 and U-2). Similar to Figure 3b, Figure 3c shows that for the July - December climate, decreased SST (SST-3) across the Central Atlantic resulted in

increasing SWE across the study area; this was accompanied by decreasing pressure over the equator (Z-1) and a mix of increasing and decreasing wind stresses across the equator.

1 April Snowpack and Pacific Ocean SST, Z_{500}, and U_{500} (First Mode)

Figure 4 shows the correlation maps between significant regions of the Pacific Ocean SST and the western U.S. 1 April snowpack at various predictor periods. The variability of Pacific Ocean SST resulted in SCF values of 43.38%, 63.49%, and 74.36% for the first mode and 29.59%, 18.90%, and 14.57% for the second mode for three SST predictor periods, respectively. Similarly, NSC values of 2.01, 2.94, and 3.87 were obtained.

Figure 4a shows that for the January - June climate, decreased SST (SST-1) near the ENSO area and decreased SST (SST-4) near the central Pacific resulted in decreasing precipitation in April in the study area. The warming SST was associated with high pressure over central North America (Z-1), which resulted in weakening of equatorial westerlies (U-3) and strengthening of the jet stream (U-4); this resulted in decreased SWE in the region. Figure 4b shows that the decreased April – September SST along the Niño 3.4 region (SST-1) was associated decreased pressure over North America (Z-3); this, in turn, was associated with decreased westerlies (U-3), resulting in an increased SWE in the study area. Figure 4c shows a decreased SST (SST-2) for the July - December climate, which was associated

with shortwave train (as shown by a red line) and significant wind regions along the Central Pacific. These connections resulted in increased SWE in the region.

Four significant Z_{500} regions in the Pacific Ocean were detected that seemed to drive variability in the western U.S. snowpack. The first region detected was over the Gulf of Alaska and Canada was similar to one identified in Grantz et al. (2005) and the second region was over the north-central Pacific Ocean; both represented the third predictor period. The third region was along the equatorial Pacific Ocean, representing the second and third predictor periods, and the fourth region was over the U.S., representing the first predictor period. A high snow results because of low-pressure winter jet streams that develop in the region. Southerly winds drive the jet streams, which brings moisture towards the Sierra Nevada Mountains, resulting in increased snowfall (Grantz et al., 2005).

1 April Snowpack and Atlantic Ocean SST, Z_{500}, and U_{500} (First Mode)

Figure 5 shows the correlation maps between significant regions of the Atlantic Ocean SST and western U.S. 1 April snowpack at various predictor periods. The variability of the Atlantic Ocean SST resulted in SCF values of 64.29%, 66.52%, and 72.53% for the first mode and 21.12%, 20.37%, and 17.59% for the second mode for three SST predictor periods, respectively. Similarly, the NSC values of 2.78, 2.72, and 3.11 were obtained.

Figure 5a shows that for the January - June climate, the decreased SST (SST-2), spanning 60˚ W to 30˚ W and 30˚ N to 45˚ N, resulted in increasing SWE in the study area. This decreased SST was related to pressure dipoles (Z-1 and Z-2) along with increasing equatorial westerlies (U-2) and decreasing jet streams (U-3). Figure 5b shows that the decreased SST (SST-3), spanning 60˚ W to 30˚ W and 30˚ N to 45˚ N, for the April - September climate resulted in increased SWE in the study area. The decreasing SST (SST-2) was related to decreasing pressure around the Central Atlantic (Z-1) and decreasing wind stresses (U-1 and U-2) over South America. Figure 5c shows similar results for the July - December climate, with a decreasing SST (SST-3) correlated with decreasing pressure around the equator (Z-1) and a mix of increasing (U-3) and decreasing winds (U-1, U-2 and U-3). This resulted in increased SWE in the study area.

1 May Snowpack and Pacific Ocean SST, Z_{500}, and U_{500} (First Mode)

Figure 6 shows the correlation maps between significant regions of the Pacific Ocean SST and western U.S. 1 April snowpack at various predictor periods. The Pacific Ocean SST variability resulted in SCF values of 50.32%, 56.73%, and 71.49% for the first mode and 26.82%, 27.28%, and 19.24% for the second mode for the three predictor periods, respectively. Similarly, NSC values of 2.18, 2.72, and 3.65 were obtained.

Figure 6a shows for the January - June climate, increased SST (SST-1, 2, and 3) resulted in decreasing SWE in the study area. This increased SST was accompanied by an increasing

pressure ridge (Z-1) over Central America, followed by increasing equatorial westerlies (U-1) and decreasing jet streams (U-2 and U-3). Figure 6b shows that for the April - September climate, increased SST in the Niño 3.4 region (SST-1) was associated with increased pressure over Indonesia, Asia, and the study area (Z-1, Z-3 and Z-4) as well as decreased pressure over the southern Pacific (Z-2) accompanied by increased equatorial westerlies (U-3). This resulted in decreased SWE in the region. Figure 6c shows increased SST for the July - December climate, along the ENSO belt (SST-1), causing decreasing precipitation in the study area. This was associated with a pronounced shortwave train (shown by red dash line), accompanied by significant wind regions over the Pacific Ocean.

The lagged SVD analysis shows a negative correlation between data for the central mid-latitude Pacific Ocean SST and SWE of the following year. This analysis was correlated with an anticyclone over the central U.S. and equatorial easterly winds. The July - December lead months correlated with an ENSO signal. This was a positive correlation between SSTs and SWE in the Cascades and northern Rocky Mountains of the western U.S. that was driven by intensified easterly winds and a pronounced shortwave train observed in the Z_{500} data. This shortwave train differed from the non-ENSO shortwave train that was identified by Wang et al. (2011), because it is shifted to the east, with its terminus over the Great Lakes region, versus ending at the Pacific Northwest coast of North America.

1 May Snowpack and Atlantic Ocean SST, Z_{500}, and U_{500} (First Mode)

Figure 7 shows the correlation maps between significant regions of the Atlantic Ocean SST and western U.S. 1 May snowpack at various predictor periods. The variability of the Atlantic Ocean SST resulted in SCF values of 68.09%, 72.64%, and 74.91% for the first mode and 20.99%, 17.24%, and 16.79% for the second mode for the three predictor periods. Similarly, the NSC values of 3.07, 3.13, and 3.39, respectively, also were obtained.

Figure 7a shows the January - June climate, in which decreased SST (SST-2) along 30˚ N longitude resulted in increasing SWE in the region. The decreased SST (SST-2) was correlated with decreasing pressure over the same region (Z-1), followed by decreasing westerlies (U-2) and a increasing jet stream (U-3). Figure 7b shows that decreasing SST along 30˚ N longitude (SST-2) was correlated with decreasing pressure over the central North America (Z-1) and increasing wind over southern North America (U-2) as well as decreasing wind over northern North America (U-3) and southern South America (U-1). This connection resulted in increasing SWE in the region. Similarly, Figure 7c shows decreased SST (SST-3) for the July – December climate, resulting in increasing SWE in the study area. The decreasing SST was strongly correlated with decreasing pressure (Z-1) across the equator, accompanied by increasing equatorial westerlies (U-1) and a decreasing jet stream (U-2).

The second region in the north central Pacific Ocean, extending from 150° E - 180° W, was found to be positively correlated with the snowpack. The region was identified in the literature as the Hondo region (Lamb et al., 2010) and linked with snowpack variability in the western U.S. along with hydrology of Asia (Zhang et al., 1997; Rajgopalan et al., 2000). Aziz et al. (2010) acknowledged that the region extending from 34° N - 24° S and 150° E - 160° W was the primary driver of snowpack variability in the western United States. The study analyzed 1 April snowpack stations in Colorado and Utah, utilizing SVD, and concluded that the Hondo region drives the snowpack. Further, the study utilized reconstruction data to corroborate their findings. Another region that is highly correlated is located near the Australian continent, and is inversely correlated with snowpack variability in the western United States. Wang and Ting (2000) acknowledged this region, and associated it with the variability of snowpack and precipitation in the U.S.

1 April Snowpack and Pacific Ocean SST, Z_{500}, and U_{500} (Second Mode)

Figure 8 shows the SST, Z_{500}, and U_{500} regions that are significantly correlated with western U.S. 1 April snowpack for the July - December climate for the second mode. A distinct SST pattern was identified near the eastern coast of Japan (SST-1) that resembles neither ENSO nor PDO. Stewart et al. (2005) studied the variability in streamflow timing by the effects of temperature, and attributed this change to PDO. This region appears to be driving

snow in stations located in Utah, Colorado, New Mexico, and Arizona that were not identified as correlated with the SST in the first mode. The relationship between SST and snowpack in Colorado and Utah was negatively correlated, which means that an increase in SST results in a decrease in snowpack in these states. The decreased SST (SST-1) was accompanied by decreasing pressure regions (Z-1. Z-2, Z-3, Z-4, and Z-5) and increasing wind velocities (U-1 and U-2). According to Rajagopalan et al. (2000), this non-ENSO like pattern has been identified by many researchers in the past. Most of the significantly correlated regions can be explained physically, based on the underlying ocean-atmospheric phenomena; other correlations are inexplicable because, under certain circumstances, SVD produces paired patterns that have no physical meaning (e.g., Newman and Sardeshmukh, 1995).

Standardized TES for the Pacific and Atlantic Oceans were plotted in Fig. 9a and b, respectively. The analysis was conducted for all the seasons with 1 April SWE in order to show the decadal variations observed in the data within the time period being considered. Each individual SVD resulted in two standardized TES, one for SST and the other for SWE. In Figure 9, standardized TES for SST is represented by a solid line and that for SWE is represented by a dotted line. The TES shows the behavior of the SST index for the entire Pacific and Atlantic Oceans.

As seen from the analysis (Figures 2 through 8), the TES shows a strong correlation with regions such as ENSO, PDO, and AMO as well as with other regions of the Pacific and Atlantic Oceans. As can be seen from the SCF and r value in Figure 9, this correlation between the TES of the Pacific (Atlantic) Ocean SST and TES of the Pacific (Atlantic) Ocean SWE shows the advantage of using SVD, which develops a relationship among all the regions of Pacific and Atlantic Oceans and the SWE. The TES obtained by utilizing current SVD techniques, taking into consideration the entire Pacific Ocean and Atlantic Ocean, could result in improved SWE predictability.

Figure 9 also shows the variability of SST and SWE within the time series that was considered. The objective of this present study was to qualify the data included in the climatological record (i.e., 1971-2010) so that future forecasts could be better informed. Forecasters must use that period for official forecasts; therefore, the TES obtained for the period being considered should be utilized by forecasters to predict the SWE in the region. Examining the entire available record may reveal longer-term patterns, but it would not help forecasters understand how to work with the tools they have.

Conclusion

This research reaffirmed results from previous studies, and provided new insights when evaluating the SVD analyses between Pacific and Atlantic SST/ Z_{500}/ U_{500} and western U.S.

snowpack. The study utilized current SNOTEL data (1 March, 1 April, and 1 May), and a lead-time approach was utilized to predict the variability of SWE in the western U.S. The use of SVD removed any assumptions of linearity or normality while analyzing the relationships between oceanic-atmospheric indices and SWE.

The main conclusions drawn in this paper are as follows.

1. Warming (cooling) of the equatorial SST near the ENSO belt, El Niño-like conditions (La Niña-like conditions) resulted in decreasing (increasing) SWE in the western U.S., excluding the states of Colorado and Utah.
2. Second mode SVD showed cooling of the SST near the Asian and Australian continents, resulting in increasing SWE in the states of Colorado and Utah.
3. Cooling of the SST near the ENSO belt was significantly correlated with a pronounced shortwave train in the Z_{500} data, which terminated near the Great Lakes and resulted in increasing SWE in the western United States.
4. Warming of the SST region near the east coast of Japan, accompanied by an increasing pressure ridge over the study area along with increasing equatorial westerlies and a decreasing jet stream, resulted in a declining SWE in the study area.
5. Decreasing SST along 30˚ N longitude in the Atlantic Ocean resulted in increasing SWE, which was correlated with a decreasing pressure ridge along the equator as well as increasing equatorial westerlies and decreasing jet streams.

The major contributions of this study are as follows.

1. Using values for SST/ Z_{500}/ U_{500} from the entire Pacific and Atlantic Oceans, over predefined regions of these indices, helped to remove spatial biases over the time period being considered.
2. The modified SVD approach utilized in the present study helped when analyzing the changes in western U.S. SWE by taking into consideration all the climate indices together. This was because the variables (SST/ Z_{500}/ U_{500}) operate together to drive the SWE into the Great Basin.

Particularly under a changing climate, it is important to understand the full context of the range of atmospheric and oceanic variabilities and their effects on water resources in the western United States. Over the past 50 years, only six strong El Niño events have been observed, based on indices developed over the Niño 3.4 region. Each of these strong El Niño events have been unique, and were characterized by a broad range of hydrologic effects to the western U.S., despite similar SSTs in the Niño 3.4 region. Despite the small sample size, these strong El Niño events commonly are used as analogs or else incorporated into resource management planning. By taking into account a broader representation of atmospheric and oceanic dynamics, the resource management community may be better able to characterize and forecast seasonal availability of their water resources.

The ability to improve forecast lead time, particularly as the effects of climate change are realized, has the potential to improve resource management, particularly as it relates to hydrologic resources. Typically, forecasts regarding water supply rely on an assumption of *stationarity*, that is, the assumption that the past climate (i.e., temperature and precipitation) would provide acceptable guidance when developing long-term forecasts of water supply and resource availability. As the results of climate change affect the characteristics of precipitation and behavior of the global hydrologic cycle, the assumption of stationarity no is longer valid.

This paper presents the correlation between SWE and oceanic and atmospheric variability. Using the information presented in this paper, forecasters and resource managers may be able to improve long-term forecasts to more accurately predict water supply conditions in those areas where snowmelt plays a significant role, for example, in the Colorado River Basin. In addition, this study considered Atlantic Ocean influences on western U.S. snowpack variability, taking into account the effects of Z_{500} and U_{500}, together with SST, in order to understand the changes in western US SWE. The present study provides numerous contributions in grasping the relationship between climate indices in the Pacific and Atlantic Oceans and the SWE in the western United States.

Several new SST, Z_{500} and U_{500} regions were detected that are significantly correlated regions. They may be utilized in forecasting models by taking into consideration additional climate indices, such as Z_{500} and U_{500}, to better represent SWE variability and manage water resources within a region. The authors recognize that a short period of data record was utilized in this study (1961-2016); in the future, this issue can be addressed by utilizing reconstructed data. Also, the mechanisms involved in SST, jet stream and pressure cannot be completely explained by statistical approach and requires understanding of climate forcing in detail on a regional/local scale.

Acknowledgments

The authors would like to thank three anonymous reviewers for their critical and constructive comments which helped to improve this manuscript. The authors would like to thank the SIU Carbondale water lab team members Balbhadra Thakur and Swastik Bhandari for their valuable suggestions during the preparation of this manuscript. The authors are grateful to Office of Vice Chancellor for Research at SIU Carbondale for providing research support. The information relating to dataset used in the analysis is provided in the manuscript.

References

Ao, J., & Sun, J. (2015). "Connection between November snow cover over Eastern Europe and winter precipitation over East Asia." *International Journal of Climatology*.

Aziz, O. A., Tootle, G. A., Gray, S. T., and Piechota, T. C. (2010). "Identification of Pacific Ocean sea surface temperature influences of Upper Colorado River Basin snowpack." *Water Resources Research*, 46(7).

Barnett, T., and Preisendorfer, R. (1987). "Origins and levels of monthly and seasonal forecast skill for United States surface air temperatures determined by canonical correlation analysis." *Monthly Weather Review*, 115(9), 1825-1850.

Bretherton, C. S., Smith, C., and Wallace, J. M. (1992). "An intercomparison of methods for finding coupled patterns in climate data." *Journal of climate*, 5(6), 541-560.

Cayan, D. R., and Peterson, D. H. (1989). "The influence of North Pacific atmospheric circulation on streamflow in the west." *Aspects of climate variability in the Pacific and the western Americas*, 375-397.

Dawadi, S., and Ahmad, S. (2012). "Changing climatic conditions in the Colorado River Basin: implications for water resources management." *Journal of Hydrology*, 430, 127-141.

Dettinger, M. D., & Diaz, H. F. (2000). "Global characteristics of stream flow seasonality and variability." *Journal of Hydrometeorology*, 1(4), 289-310.

Enfield, D. B., Mestas-Nuñez, A. M., and Trimble, P. J. (2001). "The Atlantic multidecadal

oscillation and its relation to rainfall and river flows in the continental US." *Geophysical Research Letters*, 28(10), 2077-2080.

Grantz, K., Rajagopalan, B., Clark, M., and Zagona, E. (2005). "A technique for incorporating large-scale climate information in basin-scale ensemble streamflow forecasts." *Water Resources Research*, 41(10).

Hagemann, S., Chen, C., Clark, D., Folwell, S., Gosling, S. N., Haddeland, I., & Wiltshire, A. (2013). "Climate change impact on available water resources obtained using multiple global climate and hydrology models." *Earth System Dynamics*, 4, 129-144.

Hamlet, A. F., Mote, P. W., Clark, M. P., & Lettenmaier, D. P. (2005). "Effects of temperature and precipitation variability on snowpack trends in the western United States." *Journal of Climate*, 18(21), 4545-4561.

Hunter, T., Tootle, G., and Piechota, T. (2006). "Oceanic-atmospheric variability and western US snowfall." *Geophysical Research Letters*, 33(13).

Kahya, E., and Dracup, J. A. (1993). "US streamflow patterns in relation to the El Niño/Southern Oscillation." *Water Resources Research*, 29(8), 2491-2503.

Kalman, D. (1996). "A singularly valuable decomposition: the SVD of a matrix." *The college mathematics journal*, 27(1), 2-23.

Jin, J., Miller, N. L., Sorooshian, S., & Gao, X. (2006). "Relationship between atmospheric circulation and snowpack in the western USA." *Hydrological Processes*, 20(4), 753-767.

Lamb, K. W., Piechota, T. C., Aziz, O. A., and Tootle, G. A. (2010). "Basis for extending long-term streamflow forecasts in the Colorado River basin." *Journal of Hydrologic Engineering*, 16(12), 1000-1008.

Lempert, R. J., & Groves, D. G. (2010). "Identifying and evaluating robust adaptive policy responses to climate change for water management agencies in the American west." *Technological Forecasting and Social Change*, 77(6), 960-974.

Li, R., Wang, S. Y., Gillies, R. R., Buckley, B. M., Truong, L. H., & Cho, C. (2015). "Decadal oscillation of autumn precipitation in Central Vietnam modulated by the East Pacific–North Pacific (EP–NP) teleconnection." *Environmental Research Letters*,10(2), 024008.

McCABE, G. J., & Dettinger, M. D. (1999). "Decadal variations in the strength of ENSO teleconnections with precipitation in the western United States." *International Journal of Climatology*,*19*(13), 1399-1410.

Mantua, N. J., Hare, S. R., Zhang, Y., Wallace, J. M., and Francis, R. C. (1997). "A Pacific interdecadal climate oscillation with impacts on salmon production." *Bulletin of the american Meteorological Society*, 78(6), 1069-1079.

Mote, P. W., Hamlet, A. F., Clark, M. P., & Lettenmaier, D. P. (2005). "Declining mountain snowpack in western North America." *Bulletin of the American meteorological Society*, 86(1), 39-49.

Munot, A., and Kumar, K. K. (2007). "Long range prediction of Indian summer monsoon

rainfall." *Journal of earth system science*, 116(1), 73-79.

Newman, M., and Sardeshmukh, P. D. (1995). "A caveat concerning singular value decomposition." *Journal of Climate*, 8(2), 352-360.

Oubeidillah, A. A., Tootle, G. A., Moser, C., Piechota, T., and Lamb, K. (2011). "Upper Colorado River and Great Basin streamflow and snowpack forecasting using Pacific oceanic–atmospheric variability." *Journal of Hydrology*, 410(3), 169-177.

Pachauri, R. K., Allen, M., Barros, V., Broome, J., Cramer, W., Christ, R., Church, J., Clarke, L., Dahe, Q., and Dasgupta, P. (2014). "Climate Change 2014: Synthesis Report. Contribution of Working Groups I, II and III to the Fifth Assessment Report of the Intergovernmental Panel on Climate Change."

Pathak P, Kalra A, Ahmad S and Bernardez M (2016a). "Wavelet-Aided Analysis to Estimate Seasonal Variability and Dominant Periodicities in Temperature, Precipitation, and Streamflow in the Midwestern United States." *Water Resources Management*. Doi:10.1007/s11269-016-1445-0.

Pathak, P., Kalra, A., & Ahmad, S. (2016b). "Temperature and Precipitation changes in the Midwestern United States: Implications for water management." *International Journal of Water Resources Development*, 1-17. Doi:10.1080/07900627.2016.1238343.

Rajagopalan, B., Cook, E., Lall, U., and Ray, B. K. (2000). "Spatiotemporal variability of ENSO and SST teleconnections to summer drought over the United States during the twentieth century." *Journal of Climate*, 13(24), 4244-4255.

Pederson, G. T., Gray, S. T., Woodhouse, C. A., Betancourt, J. L., Fagre, D. B., Littell, J. S., & Graumlich, L. J. (2011). "The unusual nature of recent snowpack declines in the North American Cordillera." *Science*, 333(6040), 332-335.

Rajagopalan, B., Cook, E., Lall, U., & Ray, B. K. (2000). "Spatiotemporal variability of ENSO and SST teleconnections to summer drought over the United States during the twentieth century." *Journal of Climate*, 13(24), 4244-4255.

Redmond, K. T., and Koch, R. W. (1991). "Surface climate and streamflow variability in the western United States and their relationship to large-scale circulation indices." *Water Resources Research*, 27(9), 2381-2399.

Safeeq, M., Shukla, S., Arismendi, I., Grant, G. E., Lewis, S. L., & Nolin, A. (2015). "Influence of winter season climate variability on snow–precipitation ratio in the western United States." *International Journal of Climatology*.

Sagarika, S., Kalra, A., and Ahmad, S. (2015a). "Interconnections between oceanic–atmospheric indices and variability in the U.S. streamflow." *Journal of Hydrology*, 525, 724-736.

Sagarika, S., Kalra, A., and Ahmad, S. (2015b). "Pacific Ocean SST and Z500climate variability and western U.S. seasonal streamflow." *International Journal of Climatology*, 36(3), 1515-1533.

Scalzitti, J., Strong, C., & Kochanski, A. (2016). "Climate change impact on the roles of temperature and precipitation in western US snowpack variability." *Geophysical*

Research Letters, 43(10), 5361-5369.

Soukup, T. L., Aziz, O. A., Tootle, G. A., Piechota, T. C., and Wulff, S. S. (2009). "Long lead-time streamflow forecasting of the North Platte River incorporating oceanic–atmospheric climate variability." *Journal of Hydrology*, 368(1), 131-142.

Stephen, H., Ahmad, S., Piechota, T. C., and Tang, C. (2010). "Relating surface backscatter response from TRMM precipitation radar to soil moisture: results over a semi-arid region." *Hydrology and Earth System Sciences*, 14(2), 193-204.

Stewart, I. T., Cayan, D. R., & Dettinger, M. D. (2005). "Changes toward earlier streamflow timing across western North America." *Journal of climate*, 18(8), 1136-1155.

Tamaddun, K., Kalra, A., and Ahmad, S. (2016). "Identification of Streamflow Changes across the Continental United States Using Variable Record Lengths." *Hydrology*, 3(2), 24.

Tamaddun, K., Kalra, A., Bernardez, M., and Ahmad, S. (2017a). "Multi-Scale Correlation between the Western US Snow Water Equivalent and ENSO/PDO Using Wavelet Analyses." *Water Resources Management*, 31(9), 2745-2759.

Tamaddun, K., Kalra, A., and Ahmad, S. (2017b). "Wavelet analyses of western US streamflow with ENSO and PDO." *Journal of Water and Climate Change*, 8(1), 26-39.

Thakali, R., Kalra, A., & Ahmad, S. (2016). "Understanding the Effects of Climate Change on Urban Stormwater Infrastructures in the Las Vegas Valley." *Hydrology*, 3(4), 34.

Ting, M., and Wang, H. (1997). "Summertime US Precipitation Variability and Its Relation toPacific Sea Surface Temperature." *Journal of Climate*, 10(8), 1853-1873.

Tootle, G. A., and Piechota, T. C. (2006). "Relationships between Pacific and Atlantic ocean sea surface temperatures and US streamflow variability." *Water Resources Research*, 42(7).

Trenberth, K. E. (2011). "Changes in precipitation with climate change." *Climate Research*, 47(1-2), 123-138.

Trenberth, K. E., and Hoar, T. J. (1997). "El Niño and climate change." *Geophysical Research Letters*, 24(23), 3057-3060.

Uvo, C. B., Repelli, C. A., Zebiak, S. E., and Kushnir, Y. (1998). "The relationships between tropical Pacific and Atlantic SST and northeast Brazil monthly precipitation." *Journal of Climate*, 11(4), 551-562.

Wang, H., and Ting, M. (2000). "Covariabilities of winter US precipitation and Pacific sea surface temperatures." *Journal of Climate*, 13(20), 3711-3719.

Wang, S.-Y., Gillies, R. R., Hipps, L. E., and Jin, J. (2011). "A transition-phase teleconnection of the Pacific quasi-decadal oscillation." *Climate dynamics*, 36(3-4), 681-693.

Wang, S. Y., Gillies, R. R., & Reichler, T. (2012). "Multidecadal drought cycles in the Great Basin recorded by the Great Salt Lake: Modulation from a transition-phase teleconnection." *Journal of Climate*, 25(5), 1711-1721

Yang, F., and Lau, K. M. (2004). "Trend and variability of China precipitation in spring and summer: linkage to sea-surface temperatures." *International Journal of Climatology*, 24(13), 1625-1644.

Zhang, R., & Delworth, T. L. (2007). "Impact of the Atlantic multidecadal oscillation on North Pacific climate variability." *Geophysical Research Letters*,*34*(23).

Zhang, Y., Sperber, K. R., and Boyle, J. S. (1997). "Climatology and interannual variation of the East Asian winter monsoon: Results from the 1979-95 NCEP/NCAR reanalysis." *Monthly Weather Review*, 125(10), 2605-2619.

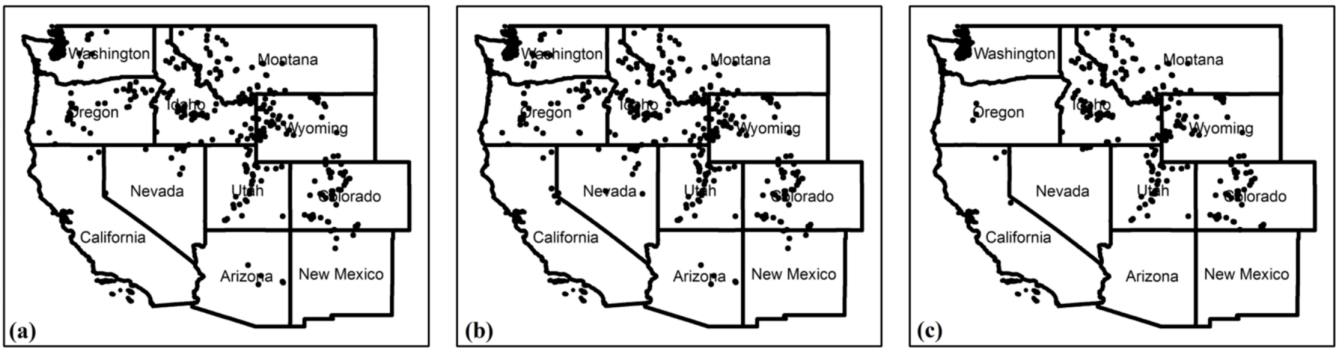

Fig 1.tif

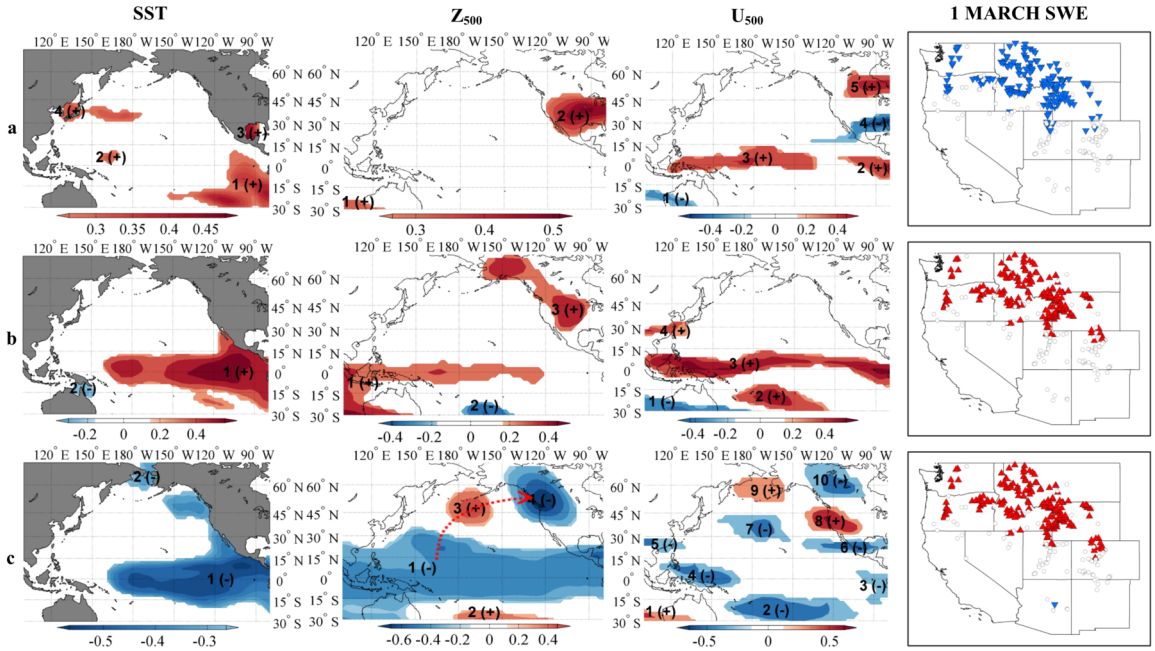

Fig 2.tif

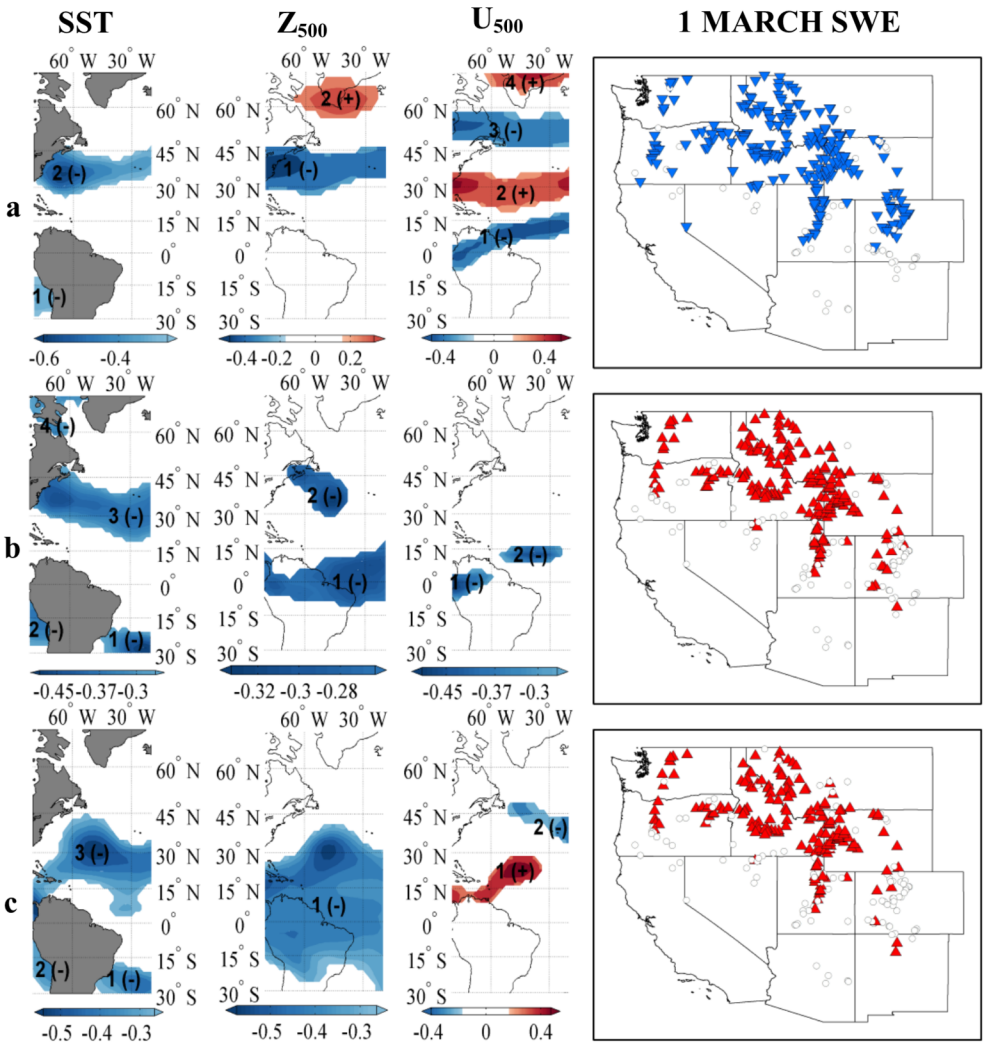

Fig 3.tif

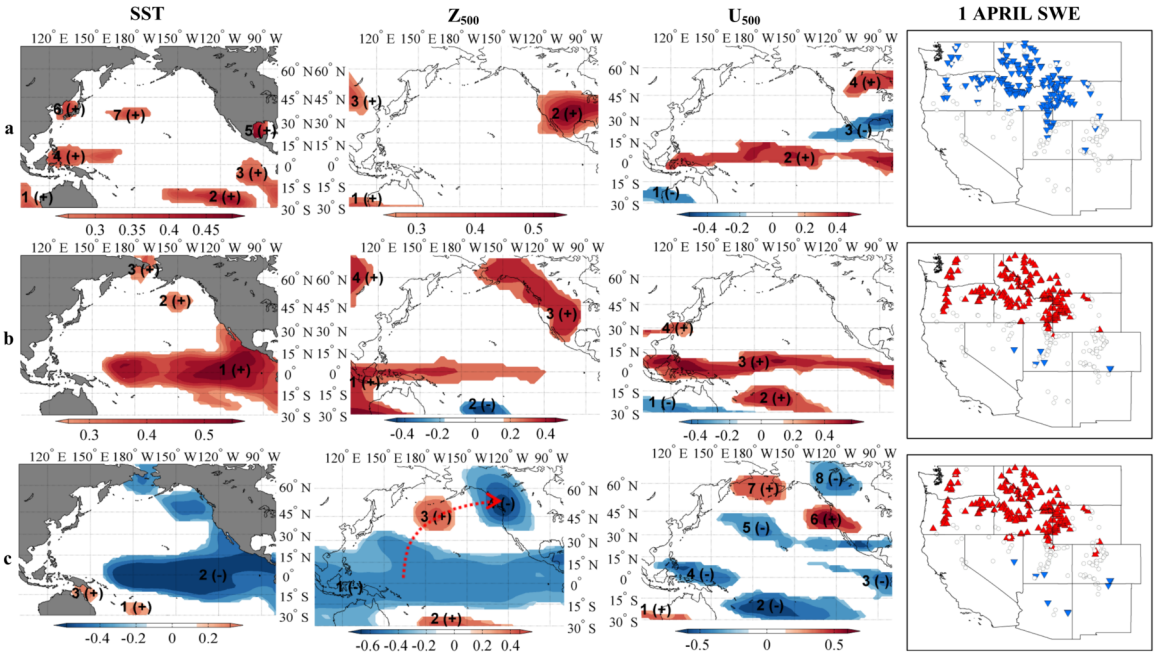

Fig 4.tif

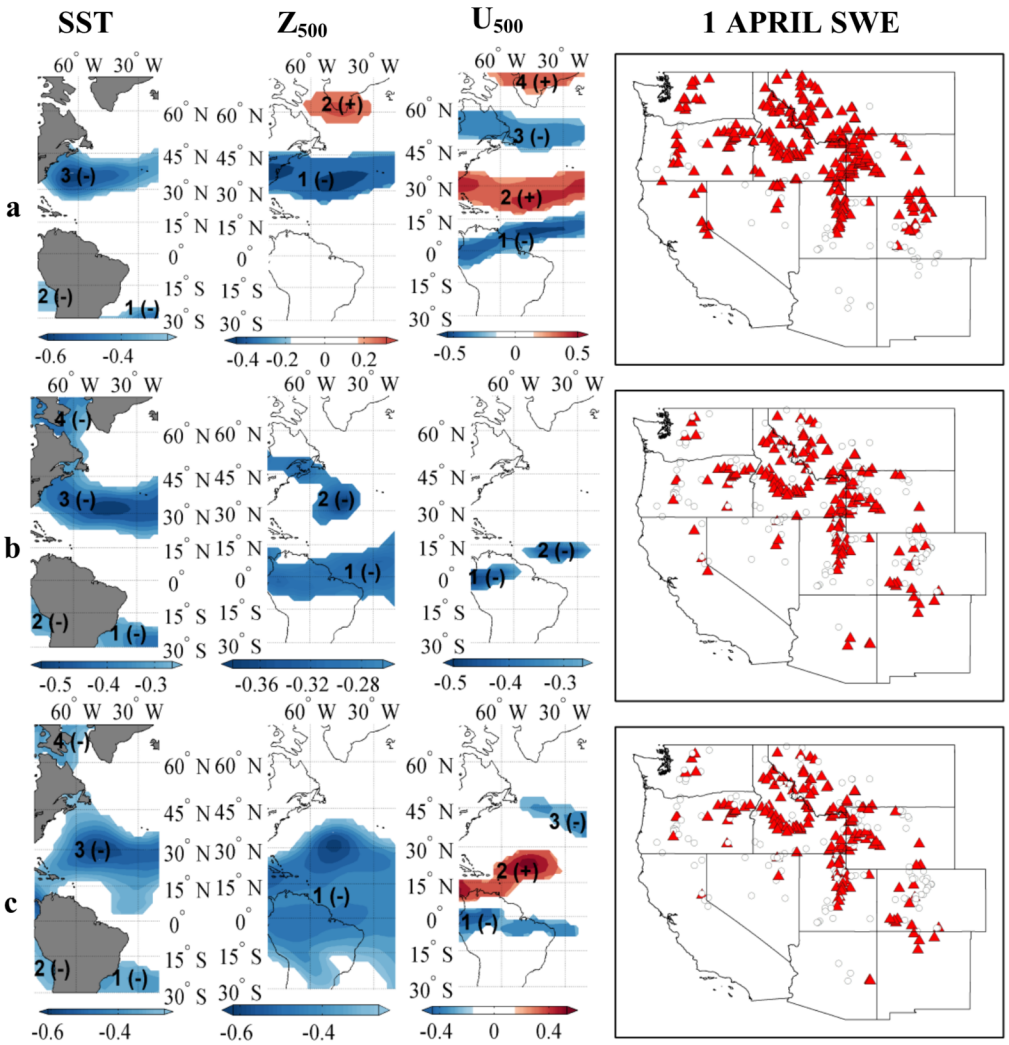

Fig 5.tif

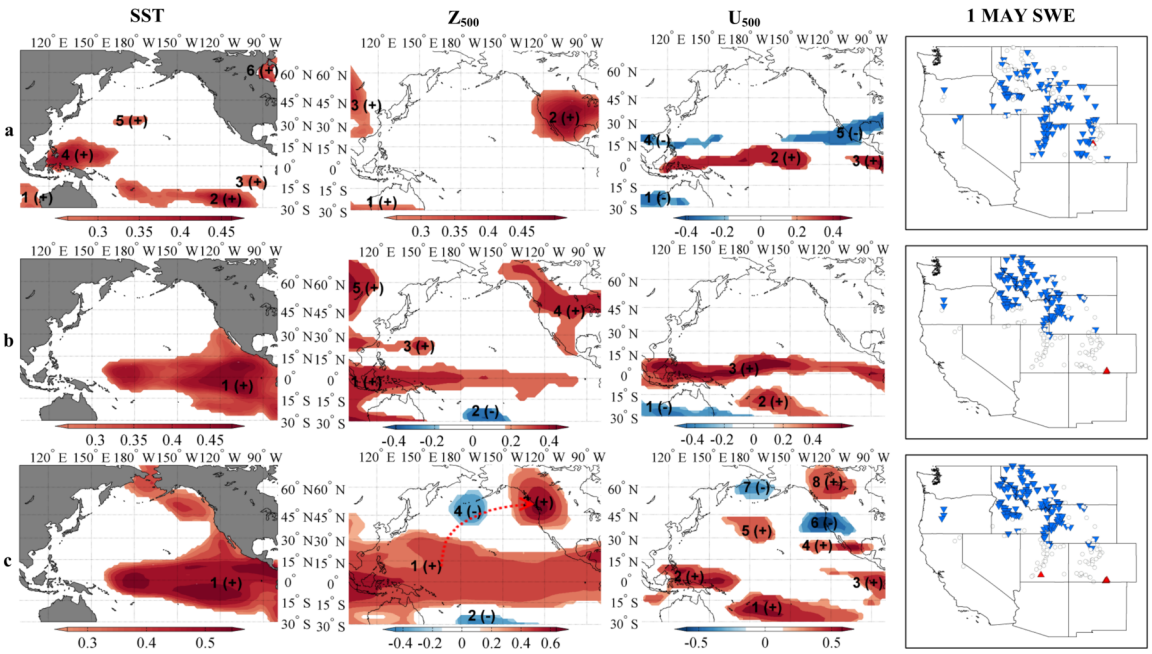

Fig 6.tif

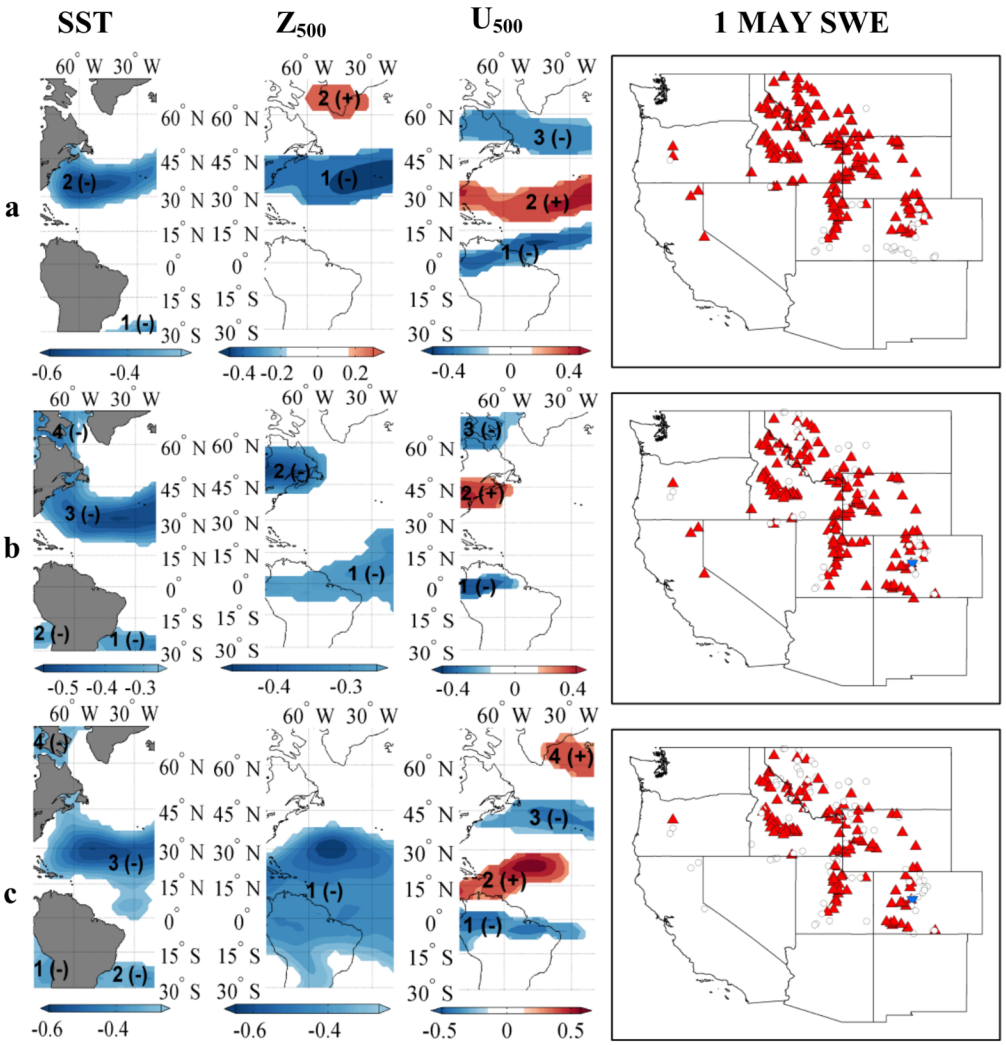

Fig 7.tif

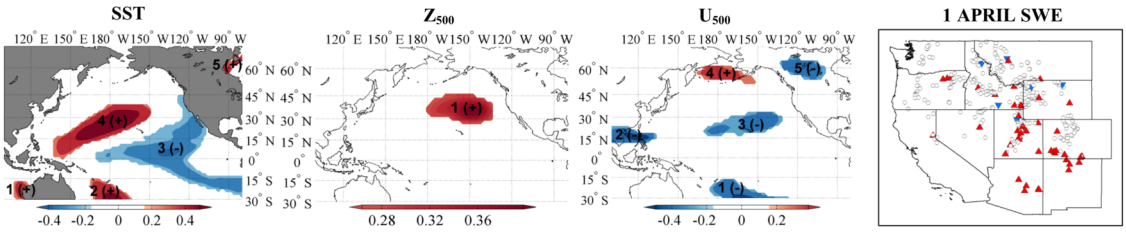

Fig 8.tif

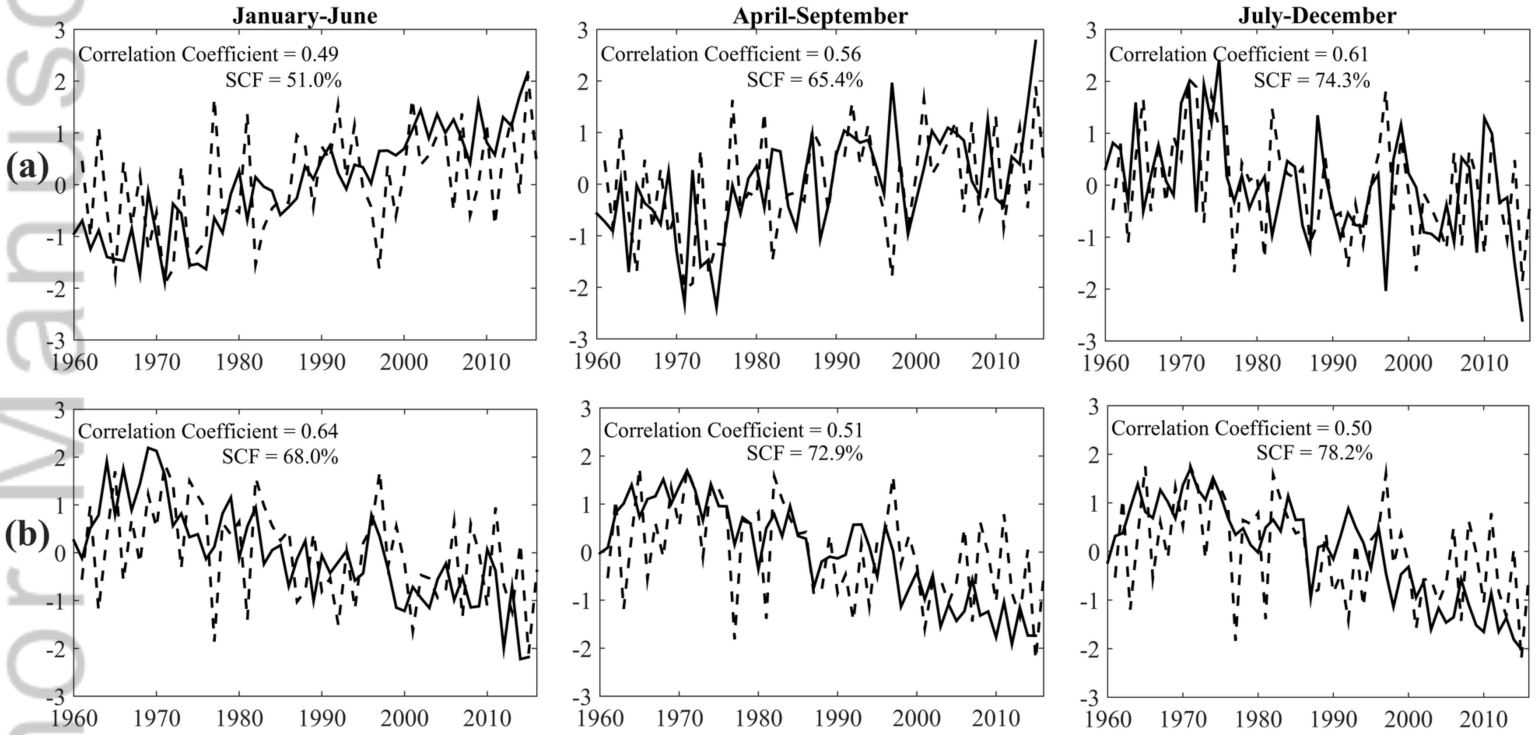

Fig 9.tif